Journal of Hydrology 629 (2024) 130561

Contents lists available at ScienceDirect

Journal of Hydrology

journal homepage: www.elsevier.com/locate/jhydrol

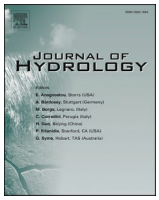

Research papers

Investigation of uniform and graded sediment wash-off in an urban drainage system: Numerical model validation from a rainfall simulator in an experimental facility

W. Addison - Atkinson [a,*], A.S. Chen [a], F.A. Memon [a], J. Anta [b], J. Naves [b], L. Cea [b]

[a] Centre for Water Systems, Harrison Building, University of Exeter, EX4 4QF, Spain
[b] Universidade da Coruña, Water and Environmental Engineering Research Team (GEAMA), Centre for Technological Innovation in Construction and Civil Engineering (CITEEC), Campus de Elviña, 15071 A Coruña, Spain

ARTICLE INFO

This manuscript was handled by Sally Elizabeth Thompson, Ph.D., Editor-in-Chief, with the assistance of Lauren E. McPhillips, Associate Editor

ABSTRACT

Understanding sediment wash-off in urban environments plays an essential role in sediment transport management; and is critical for accurate pluvial flood control to assist in adaptation and mitigation strategies. Sediment transport models have been researched previously, though challenges still arise due to the complicated nature of graded sediment transport. This study tested the accuracy of the van Rijn model using a sparse distribution of particle sizes using the geometric mean. As such, this study used high-resolution datasets collected in a water laboratory to investigate sediment wash-off and transport on an urban street. This included the interaction of two gully pots receiving sediment loads that were washed off from a hypothetical urban surface by three rainfall intensities. The results showed that the model was able to simulate uniform sediments entering the gully pots accurately when the sediment size was assigned to a median diameter. Using the grain diameter to represent the geometric mean can improve the model performance for simulating a graded sediment.

1. Introduction

Pollutant wash-off from urban surfaces is a significant environmental challenge that many urban regions endure; as this diffuse pollution source contains sediments, nutrients, bacteria, oil, metals, and chemicals (Gao et al., 2011; Muthusamy et al., 2018). This problem is exacerbated due to expanding urban populations and changes in land use (Butler et al., 2018). The development of impervious surfaces intensifies runoff volumes, and discharges entering drainage systems. This phenomenon will increase total loads and peak concentrations of suspended sediments, which can lead to blockages of sewer inlets and increased flood risk. Coarser sediments (non-cohesive) are more likely to contribute to a reduction of the performance of sewer systems, as they can restrict flow, and are less likely to be transported. Whilst finer sediments (cohesive) may cause pollution to aquatic environments, as deposition in gully pots is less likely, and chemical bonding maybe present (Deletic, 2000). For example, heavy metal pollutants in urban drainage systems are present through the attachment on finer particles. Suspended load sediments are therefore carried through the drainage system, and conveyed to receiving waters by surface runoff during flood events (Chang et al., 2019). Three main sediment wash-off processes transpire, namely sediment build up, wash-off and transport (Egodawatta et al., 2007). Sediment wash-off and sediment transport develop from rainfall-runoff processes; though rainfall intensity, rainfall energy, sediment properties, particle size, runoff-shear stress and surface type will determine how extreme the consequences of wash-off are. This is a very convoluted process; as surface type has many factors to consider; including surface texture, flow pathways, roughness, depression storage and micro-topography (Zhao et al., 2018).

Sewer blockages attributable to non-cohesive sediment wash-off can be studied by combining hydrodynamic modelling approaches with sediment transport models. Numerical models therefore play an important role in predicting blockages from sediments by simulating these complex interactions. Sediment transport models use mathematical formulas to replicate sediment wash-off processes (e.g., sediment build up, wash-off and transport). As such, many models exist in differing amounts of complexity. One drawback to the numerical modelling framework is a lack of robust data for model calibration and validation. This is due to the hostile environment of drainage systems and associated inundated regions. Other considerations include the

* Corresponding author.
E-mail address: wa259@exeter.ac.uk (W. Addison - Atkinson).

https://doi.org/10.1016/j.jhydrol.2023.130561
Received 6 June 2023; Received in revised form 21 September 2023; Accepted 12 November 2023
Available online 8 December 2023

complex nature of urban drainage systems (e.g., uncertainties in rainfall variability, sediment transport mechanisms, heterodispersity of sediment fractions and organic matter (Liu and Sansalone, 2020)). As a result some previous studies have investigated complex 2D flow regimes by validating hydrodynamic models against experimental facility datasets (Kesserwani et al., 2015; Fraga et al., 2017; Rubinato et al., 2017, 2018; Martins et al., 2017). Other studies have used experimental/laboratory facilities for validating soluble pollutant transport simulations (Beg et al., 2020; Zhang et al., 2020; Rubinato et al., 2022). Others have used surveillance cameras and crowd sourced video footage to investigate flood depths and flow velocities in field observation studies (Le Boursicaud et al., 2016; Leitão et al., 2018).

Muthusamy et al. (2018) used an experimental setup to study the effects of rainfall intensity, surface slope and initial sediment loads on sediment wash-off. They found that washed-off sediment loads are indeed proportional to rainfall intensity and the slope of the flooded surface. Additional observations included that rainfall events have the capacity to mobilise only a fraction of sediment from road surfaces. Once this capacity is reached, wash-off becomes almost zero, even though a sizable fraction of sediment is still presented on the surface. Similarly, Zhao et al. (2018) found that particle size is important factor in the wash-off process. The authors used field observations and an experimental facility to observe sediment particle sizes. They concluded that finer particles have a higher wash-off percentage than coarser particles, as their study hypothesised. Though accumulation rates are more likely to arise from vegetation factors and rainfall volume in gully pots (Rietveld et al., 2020). Nevertheless particle size will likely contribute to accumulation percentages, as seen in the work by Hong et al., (2016a).

The above-mentioned sediment wash-off studies are entirely experimental and have not compared their results with numerical simulations. Though such studies do exist. Naves et al., (2020a) used a 2D model (Iber) coupled to a Hairsine-Rose Soil Erosion Model (H-R) to conduct a sensitivity analysis (multiple linear regression analysis and Extended Fourier Amplitude Sensitivity Test) based on a series of laboratory experiments. Three rainfall intensities (30, 50 and 80 mm/h) were used against four sediment distributions (104.0 g/m^2, 13.3 g/m^2, 2.6 g/m^2, and 0.6 g/m^2). Peak concentrations of total suspended solids were highly sensitive to critical mass. Similarly, the initial load of sediment and the mean grain size were the most important variables, which usefully highlights the need for very accurate measurements. The results show the importance of sensitivity analysis due to the complex nature of model calibration. Similarly, future studies may only want to use these sensitive parameters, to simplify the modelling process.

Hong et al., (2016b) used the H-R model coupled with FullSWOF (Full Shallow Water equations for Overland Flow), to study a small urban French catchment. 21 rainfall events with different intensities were studied. Interestingly, the authors found that flow driven detachment was less important than settling velocity, sediment initial loads, and raindrop driven detachment for sediment wash-off from a sensitivity analysis (Elementary-Effects method). It is likely that flow driven detachment was less significant than the other study mentioned (e.g., Naves et al., 2020a), as effective stream powers were distinct in each study. Hong et al. (2019) then introduced Sobol's method for the sensitivity analysis and found the results to be similar. These previous numerical studies suggest that particle size removal is influenced by rainfall intensity, be it from rainfall or flow driven detachment processes. Therefore, large particles can even become detached and transported into gully pots during heavy rainfall, which can cause blockages to inlets. Initial sediment loads, sediment distribution and median diameters also play an important role. These studies have contributed to the understanding of sediment wash-off processes. Though limitations occur due to the H-R model being originally developed for rural catchments. Hence why many variables make it challenging to calibrate such models. Other uncertainties arise from the very random process of sediment build-up, so more research in this field is required. The importance of the effect of non-uniform sediment mixtures has also been studied by Xiao et al. (2022) in a small rainfall simulator. These authors found that for sediments with a D_{50} greater than 100 μm, the dominant factor in sediment transport is sediment grading.

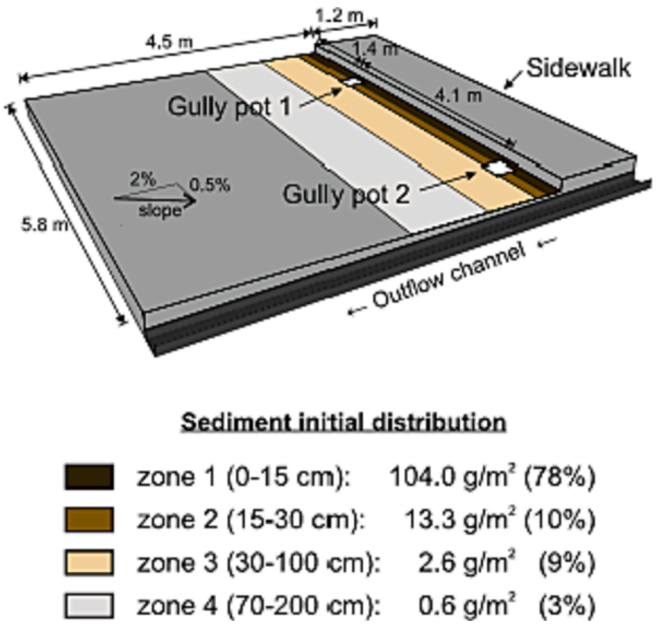

Fig. 2.1. Physical model and sediment distribution (Naves et al., 2020a).

The novelty of this paper is to use the geometrical average for graded sediment wash-off simulations with a uniform sediment model. Therefore, the aim of this present study is to contribute to the understanding of sediment wash-off in gully pots. This entails validating a new hydrodynamic model and sediment transport model in MIKE21 FM, against a dataset produced from controlled experiments in an experimental facility (Naves et al., 2017, 2020b). This study intends to use a van Rijn sand transport model to calculate sediment wash-off from the street profile. Such models are usually applied to marine environments and river systems. Though, with the correct input parameters added and initial conditions set accordingly, the model can be used for several applications. For example, the van Rijn method has been successfully implemented to study sediment transport and land erosion caused from irrigation (Darama et al., 2021), the efficiency of storm water sedimentation tanks in urban run-off (Maike et al.,2019) and sewer pipe sediment transport (Murali et al., 2019).

To our knowledge this is the first time that the sand transport model in MIKE21 FM has been applied to analyse sediment wash-off in storm water within an urban catchment; using a high-resolution experimental dataset for calibration and validation purposes. Thus, this research aims at identifying the effect sediment wash-off has on discharges entering two gully pots. The sediment transport model was calibrated using three individual uniform sediment classes of differing particle size distributions ranging from 98 to 274 μm (D2, D3 and D4). Then, the model was validated against a sediment class of 165 micros that is graded (D5), which represents a more realistic distribution of sediment. Previous tests demonstrated that the model was not able to simulate the runoff assuming the mean diameter. This is due to the mechanics of sediment transport. For example, non-cohesive sediments particles of differing sizes have opposing entrainment rates and settling velocities. This means that finer particles will have a greater wash-off percentage than coarser particles (Bui et al., 2019). Therefore, we tested the hypothesis of geometric mean diameter (D_g) of a graded sediment and quantified the improvements.

As such, the geometric mean diameter will be used as the grain diameter to simulate the graded sediment in place of medium grain size. The aim is to investigate whether the geometric mean can be applied to

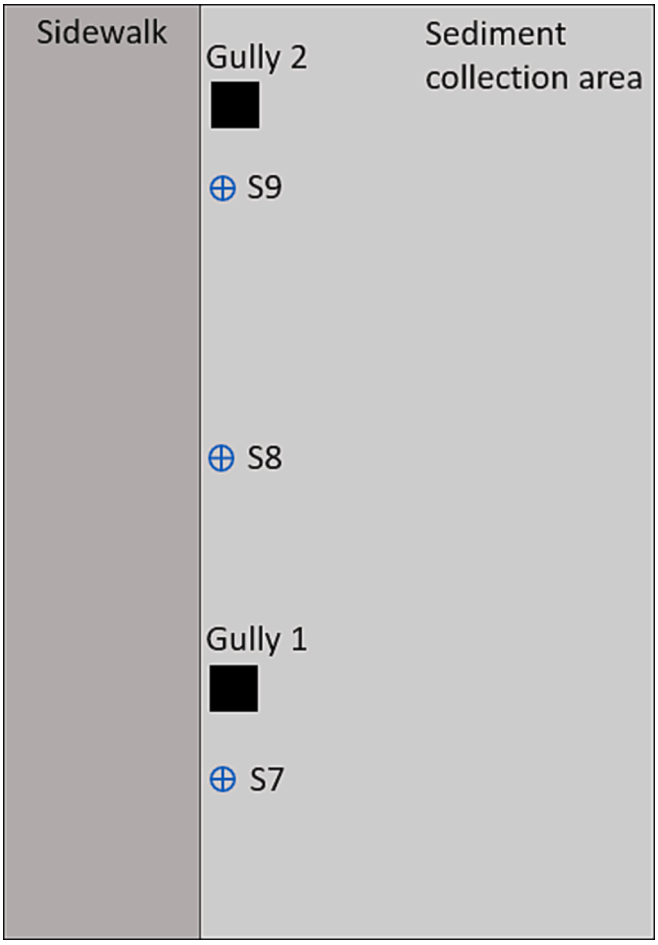

Fig. 2.2. Location of the depth measurements (S7, S8 and S9). The figure shows both gully pots, the sidewalk and sediment collection area.

accurately simulate sediment wash-off processes from a graded sediment.

2. Material and methods

2.1. Physical model description

Hydraulic data (surface depths, flows and velocities), wash-off tests (total suspended solids and particle size distribution) and rainfall intensities (30, 50 and 80 mm/h) were obtained using a full-scale physical model (This is schematically represented in Fig. 2.1.). Built in the Hydraulic Laboratory of CITEEC at the University of A Coruña Spain, this unique experimental facility has been used for multiple studies (Fraga et al., 2017; Naves et al., 2017, 2020a; Naves et al., 2019a). The model comprises of a hypothetical full scale street profile which has an area of 36 m^2. The width of the physical model is 5.8 m and the length is 4.5 m. Directly above the surface (at 2.6 m) a rainfall generator is located (Naves et al., 2020b). The rainfall generator consists of two piped circuits with 2500 pressure-compensating irrigation drippers (PCJ-CNL, Netafim^{TM}). One piped circuit allows to generate rainfall intensities of 30 and 50 mm/h. If both circuits are used simultaneously an intensity of 80 mm/h is achieved. Then, it was identified from preliminary experiments that 5 min is enough to detect the peak and the tail of the pollutographs. To allow for reliable rainfall uniformity and drop size distribution, the raindrops are broken and spread via a metallic mesh (mesh size is 3 mm), located 0.6 m below the drippers. The street surface comprises of a road (made from concrete), which is gently sloped (2 %) towards a curb. Two gully pots are located 0.02 m next to the curb. The dimensions of each gully are 0.3 m x 0.3 m. The generated rainfall drains into each gully and through a piped system to an outfall via an outflow channel. All the data files that were used in this project along with experimental details are fully open access and can be found in the WASHTREET dataset (Naves et al., 2019a, 2019b).

2.2. Experimental facility tests

Experiments consisted of simulating the three different rainfall rates (30, 50 and 80 mm/h) for a five-minute period. Measurements were recorded from when the rain started to five minutes after it stopped. This included surface flows, depths, and gully pot discharges. Surface flows were obtained using Large Scale Particle Image Velocimetry (LSPIV) techniques. This method is a common way to characterise 2D velocity fields of surface flow (Fujita et al., 1998). The water discharge into the gully pots and surface depths were measured by triangular weir and an ultrasonic distance sensor (UB500-18GM75-I-V15, Pepperl and Fuchs). Three surface depths were recorded (S7, S8, S9), which is identified in Fig. 2.2.. A total of five particle size distributions (D1-D5) were investigated in the wash-off testing. Granulometries were measured by a laser coulter particle size analyser (Beckam-Coulter LS I3 320) as seen in (Naves et al., 2019b). The initial sediment load was 20 g per meter to the curb. The sediments were realistically distributed over the roadway in different amounts. 78 % of the sediment was positioned within the first 0.15 m to the curb. 10 % and 9 % of the sediment was positioned at 0.15 m and 0.70 m, respectively; and the rest of the sediment was distributed over the rest of the surface (Fig. 2.1. shows the initial distribution of sediments). Each rainfall event was combined to a sediment wash-off test. After each experiment was performed the remaining sediment on the surface was collected. A mass balance was then performed to each particle size distribution. Structure (SfM) photogrammetric techniques were used to verify the surface elevations to raw data files such that the experiments could be replicated in the numerical modelling. More details can be found in the papers provided by Naves,et al., (2019a) and Naves et al., (2019b).

2.3. Numerical model

2.3.1. Hydrodynamic model

In this study the hydrodynamics were simulated using MIKE21 FM (DHI, 2022), which solves shallow water equations using an explicit finite volume solver on an unstructured mesh of triangles and quadrilateral elements of different sizes. Which allows it to improve the resolution in the study area whilst not increasing computational times. MIKE21 FM was used in this research as it is a robust numerical model that is very popular in academic and water industries. It is also directly linked to ESRI products (ArcGIS) and has a large free open-source python library (MIKIO). Each rainfall scenario was added individually to the hydraulic simulations, which were 30, 50 and 80 mm/h. This was implemented from 50 cm resolution rain raster files (located in the WASHTREET dataset). The unstructured mesh was created using the raw data files that were obtained from SfM topography (Fig. 2.3.). The mesh size was established after a preliminary mesh convergence analysis in which 2995 nodes and 5680 elements were used. Three open boundaries (representing locations with low elevations where water can freely flow from the domain) and one closed boundary (representing locations where the elevation is high stopping water from freely flowing over the boundary) corresponding to the street curb were used in this study. The open boundaries were set around the edge of domain (along three edges) and around each gully pot. The closed boundary was set to where the curb was located (Fig. 2.4.). The open boundaries are shown by the purple line around each gully pot and the yellow line on the outer perimeter.

2.3.2. Sediment transport model

MIKE21 FM includes the sand transport module (STM), which is

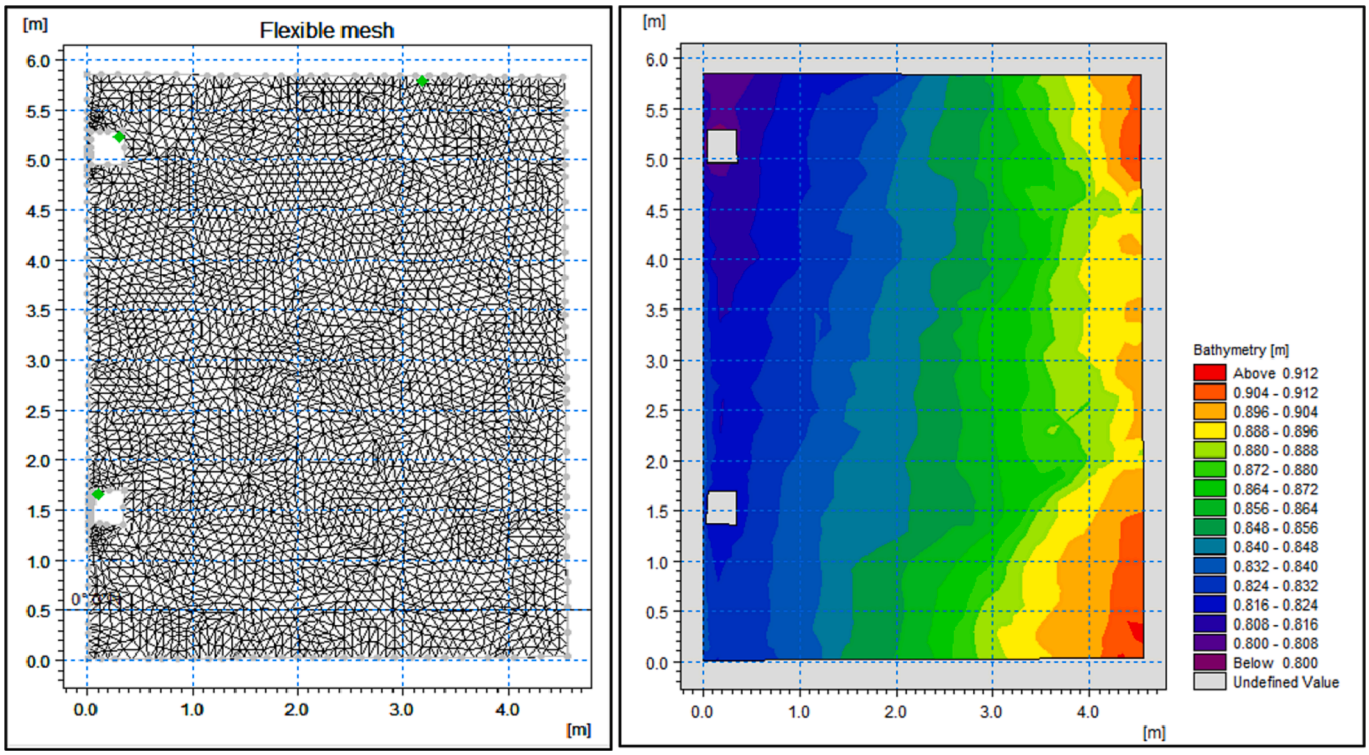

Fig. 2.3. MIKE21 FM unstructured mesh (left) and the MIKE21 FM domain (right) created from the SfM dataset, showing both gully pots.

coupled to the flow model, to simulate sediment removal, transport, and deposition under pure currents. This research used the newest version of the STM available at the time, which was under the 2022 licence. Though this has since been updated (DHI, 2023). This model has been previously applied to rivers, estuaries, and coastal areas (Sravanthi et al., 2015; Zavattero et al., 2016; Pradhan et al., 2020), though has never been used in urban catchments. The STM calculates the morphological differences for non-cohesive sediment based on the hydrological flows. The capacity of sediment transport and initial levels of bed level change are also considered. The bed load and suspended loads were calculated individually. Bed shear stress controls the bed load calculations, which will react immediately with the flows. However, there is a small phase-lag in the suspended load simulations associated to the flow, as it takes several timesteps or spatial steps to modify the vertical sediment concentration profile to the hydrodynamics. This is the transport of non-cohesive material established on average horizontal flows observed in the hydrodynamic calculations. The van Rijn equations (1989) were applied to the bed load and suspended loads of sediments. The van Rijn (1989) formula are expressed as the sum of bed load transport and suspended load flux, which is combined over depth. The bedload and suspended loads are independently computed. Sediment bed load transport (S_{bl} m^2/s) is defined in Eq. (1).

$$S_{bl} = 0.053 \frac{T^{2.1}}{D^{*0.3}} \sqrt{(s-1)g \bullet D_{50}^3} \quad (1)$$

whereby T defined in Eq. (2), is the non-dimensional transport stage parameter, which considers the critical ($u_{f,c}$) and effective (u_f) friction velocities. The effective friction velocity identifies resistance using the Chezy number, originating from skin friction which is based on logarithmic velocity profiles. This takes into consideration bed roughness values. D^* which is defined in Eq. (3), is the non-dimensional particle parameter and considers kinematic viscosity. s is the relative density of the sediment. g and D_{50} relate to gravity and median sediment diameter, respectively.

$$T = \left(\frac{u_f}{u_{f,c}}\right)^2 - 1 \quad (2)$$

$$D* = D_{50}\left(\frac{(s-1)g}{v^2}\right)^{\frac{1}{3}} \quad (3)$$

The depth integrated transport of suspended load (S_{sl} m^2/s) can be seen in equation (4). Whereby f is the relation between the depth-averaged sediment concentration and the concentration at the bed level; c_a is equal to the volumetric concentration at the bed level; V is the depth-averaged velocity (m/s), and h is the flow depth.

$$S_{sl} = f \cdot c_a \cdot V \cdot h \quad (4)$$

2.3.3. Sediment classes

Sediment class attributes were entered into the model building. This involved creating and adding external files to allow the sediment distributions to change across the domain, replicating the physical data. Each sediment class had particle size distributions as seen in Table 2.1.. The gradation coefficient ($\sigma_g = \sqrt{D_{84}/D_{16}}$) and geometric mean diameter ($D_g = \sqrt{D_{84} \bullet D_{16}}$) is also shown. A graduation coefficient close to 1 identifies a uniform sediment, and greater than 2 identifies a graded sediment. This research only investigated sediment classes D2, D3, D4 and D5 because the van Rijn equation used in the STM in MIKE 21 was calibrated for sands, thus D1 with $D_{50} < 60$ μm was not included in the analysis. Fig. 2.5. illustrates the particle size distribution of sediment classes.

2.3.4. Model calibration and analysis

Calibration of the hydrodynamic model included changing Manning's roughness (n) as bed resistance/surface roughness inputs. A value of 0.017 was then set as the roughness value. A default porosity value of 0 was kept for the simulations. Critical shear stress was left as default as changing this value was negligible on sediment transport during calibration, due to very shallow depths and small computational times. Post

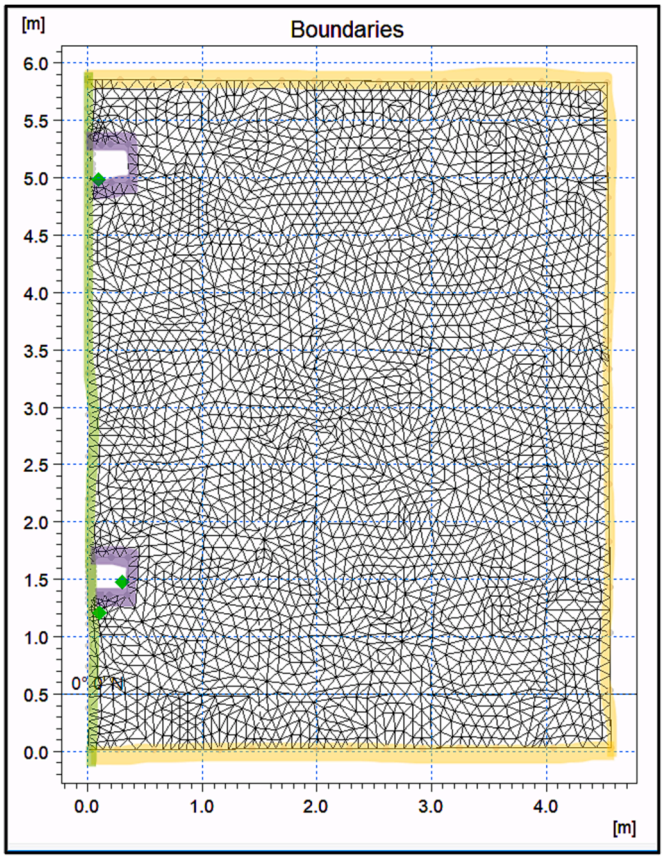

Fig. 2.4. The boundary locations used in the modelling. The open boundary is shown by the yellow line and the purple line around each gully pot. The land boundary is represented by the green line. (For interpretation of the references to colour in this figure legend, the reader is referred to the web version of this article.)

Table 2.1
Sediment classes (D1-D5) and their granulometries (D_{50}, D_{16}, D_{84}, D_g and σ_g).

Class	D_{50} (μm)	D_{16} (μm)	D_{84} (μm)	D_g (μm)	σ_g (-)
D1	30.1	11.4	54.6	25.0	2.2
D2	98.9	69.8	131.8	95.9	1.4
D3	143.9	105.8	186.8	140.5	1.3
D4	273.9	204.7	351.9	268.4	1.3
D5	165.3	48.1	291.6	118.4	2.5

model calibration, the numerical models' results were compared to the datasets collected from the physical model. This included identifying how close the numerical model was able to replicate hydraulic characteristics and sediment transport. Simulated gully pot discharges, surface velocity fields, and surface water depths of the sediment collection area were compared with the experimental datasets. Data were selected from the modelling output in a grid within the sediment collection area and compared with the experimental measured data. The results were interpolated within the mesh to that same grid then plotted each pair of points. Linear regressions to identify R^2 values of simulated and observed velocity fields within the sediment collection area were done in the x and y directions. Normalised root mean square error (NRMSE) and R^2 was also used to identify model performance regarding gully pot discharges, depths in the sediment collection area and sediment wash-off. NRMSE was acquired by dividing the root mean square error by the absolute mean of measured data. Thus, a simulation is considered excellent if the NRMSE value is less than 10 %, considered good if the value is between 10 % and 20 %, fair if the value is above 20 % and it is considered poor if the value is above 30 % (Gao et al., 2022).

3. Results

This result section compares the numerical model simulation outputs against the experimental facility dataset, with regards to gully pot discharges, surface velocity fields, surface water depths and sediments collected in the gully pots.

3.1. Gully pot discharges

The results of both gully pot discharges in all three rainfall intensities are shown in Fig. 3.1. below. The initial surge and volumetric flow rate was greater in gully 2 due to the surface slope allowing water to enter at a faster rate than gully 1. The figure illustrates the simulated and observed discharges entering gully pot 1 and 2 over the ten-minute period, respectively. In these figures simulated (sim) and observed (obs) results are shown in all three rainfall scenarios across the simulation period. Appendix A (Table A1.) also shows the R^2 values. The simulated results show that gully pot 1 had a better fit to the observed values than gully pot 2. Ranges of R^2 values for gully pot 1 and 2 were 0.95 – 0.96, and 0.93 – 0.95, respectively. The modelling results indicated that NRMSE for gully pots slightly decreased with heightened rainfall intensity, though this difference in error was very small. This is also identified in Appendix A (Table B1.); which shows the associated errors of the gully pot discharge simulations using NRMSE as the indicator. The rise and fall of flow had very good agreement, though the numerical model slightly under calculated peak discharges. The simulated gully pot NRMSE were between 12 % and 13 %.

3.2. Velocity fields from sediment collection area

The results of simulated velocities taken in the sediment collection area are shown below in Fig. 3.2.. Each rainfall scenario is shown in both velocity field directions (x and y). R^2 values are shown in Appendix A (Table A1.). Simulated velocity fields in longitudinal and lateral flows had a very good agreement against the measured data. R^2 values of longitudinal flow ranged between 0.92 and 0.91. R^2 values of lateral flows ranged between 0.92 and 0.90.

3.3. Water depths in sediment collection area

The results from water depths in the sediment collection area are shown in Fig. 3.3.. The figure illustrates the depth locations (S7, S8 and S9) and rainfall scenarios (30, 50 and 80 mm/h). Appendix A (Table B1.) also identifies the NRMSE of each location. Location S8, which is central to the surface had the highest error. Though depths closer to gully 2 (S9) were more accurate in the simulations than gully 1 (S7) since there are technical issues with measuring the depths of shallow flows, with the impact of rain generation creating turbulence. So, this is considered a good agreement due to these uncertainties.

3.4. Sediments collected in gully pots

The results of sediment wash-off into each gully pot are shown below in Fig. 3.4.. The figure compares both the simulated and observed results of particle distributions D2 - D4. The associated NRMSE for sediment wash-off for D2 - D4 were all below 12 % when using D_{50}. Further to this, D2 - D4 sediments have a very uniform granulometry, meaning that D_g and D_{50} are very similar. This meant that the simulations did not significantly vary when using D_g. Though when the graded sediment particle size distribution was simulated (D5) errors were much higher when using D_{50}. As shown in Fig. 3.5. below, which illustrates the results of the D5 particle distribution simulations. The NRMSE associated with D5 were between 43 % and 61 %. This outcome was hypothesised due to the conflicting settling velocities of sediments within non-uniform

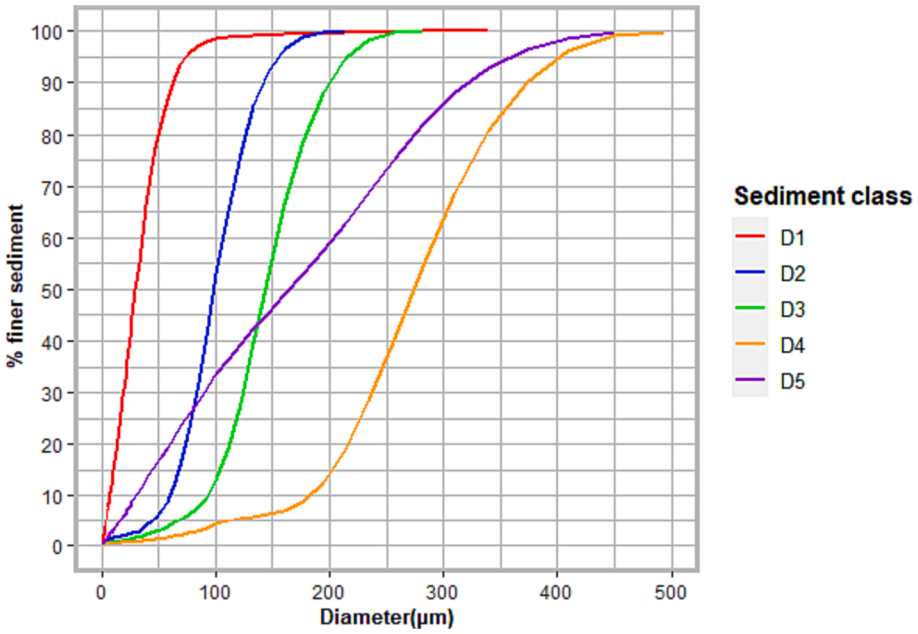

Fig. 2.5. Particle size distribution of sediment classes (D1-D5).

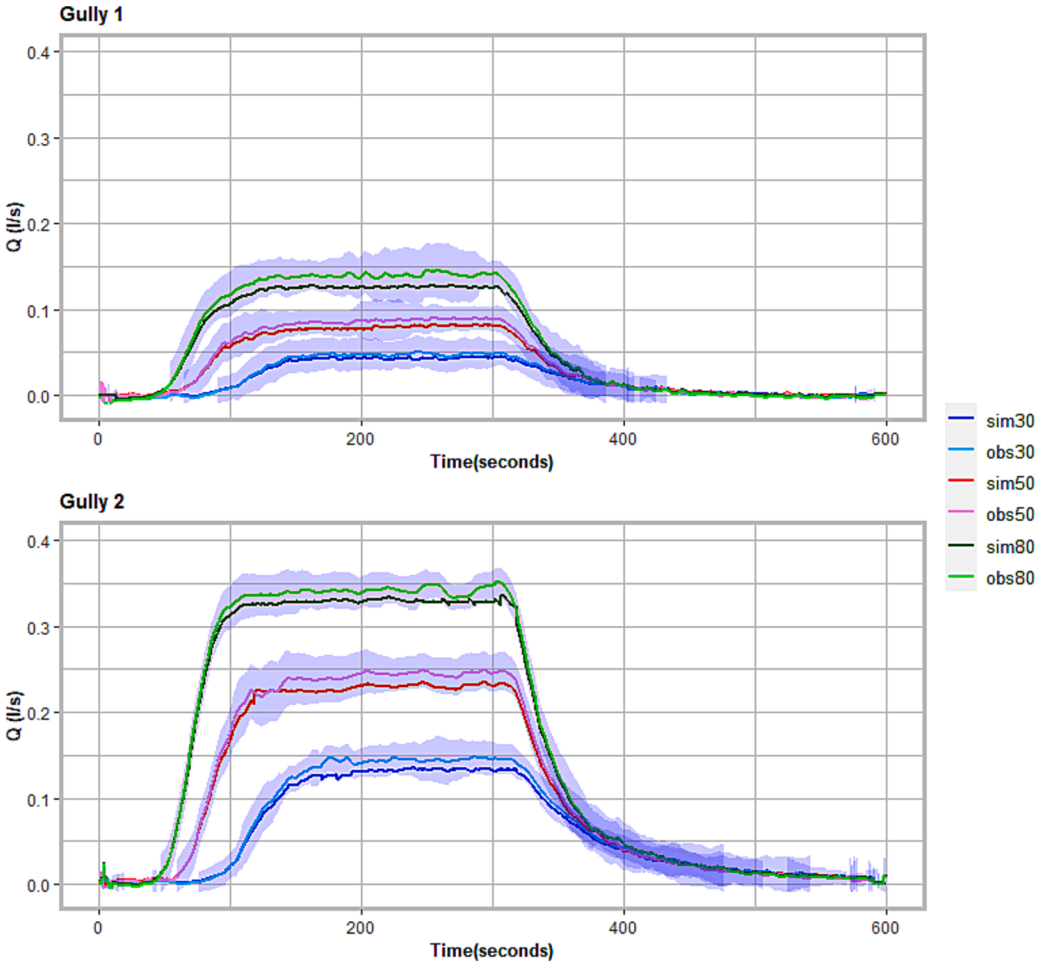

Fig. 3.1. Gully pot 1 and 2 Q (l/s) showing simulated (sim) and observed (obs) for each rainfall intensity (30, 50 and 80 mm/h). The error that is associated with the discharge determination in the testing facility is shown in the light blue ribbon. (For interpretation of the references to colour in this figure legend, the reader is referred to the web version of this article.)

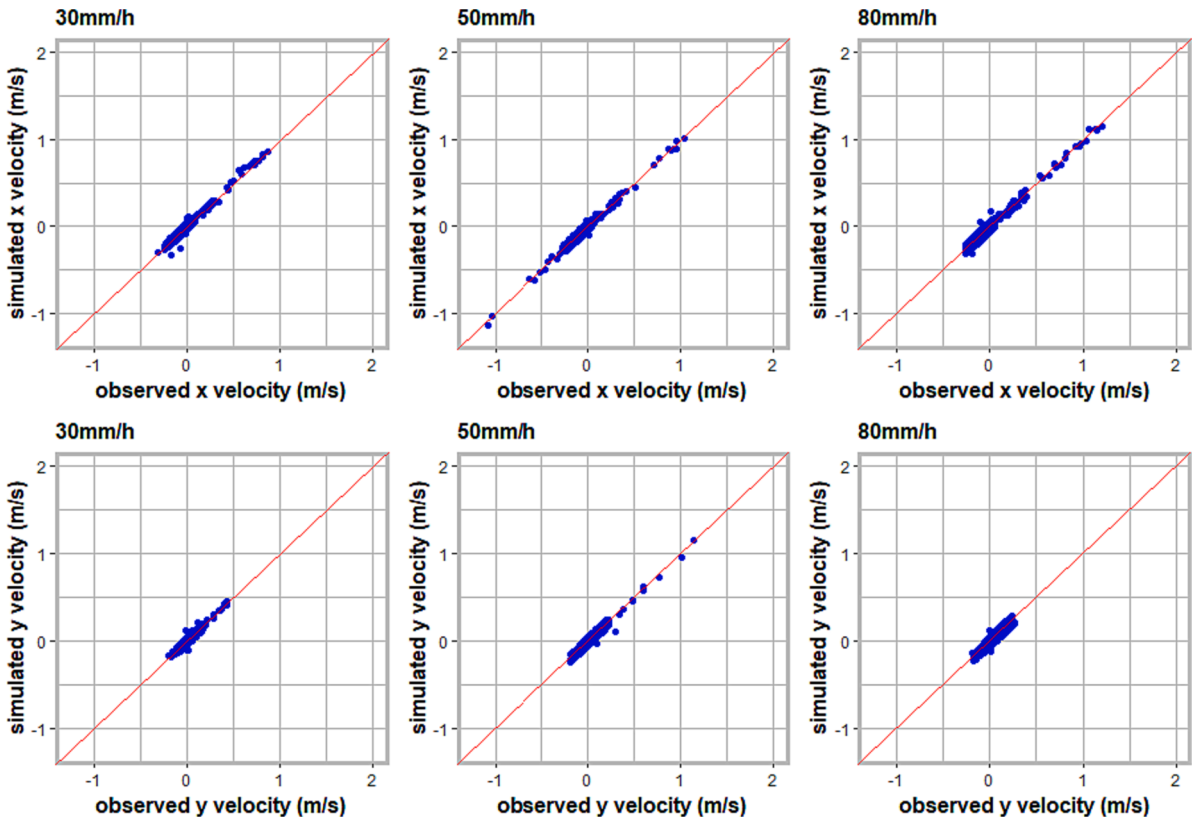

Fig. 3.2. Comparison of observed and simulated x and y direction velocities for each rainfall rate (30, 50 and 80 mm/h). Results show the velocities taken in the sediment collection area.

distributions. Fig. 3.5. also shows the results of the geometric mean simulations. The results suggest that model accuracy improved when $D5_g$ (118.4 μm) was used for the sediment diameter. NRMSE for $D5_g$ ranged between 13 % and 14 %. Appendix A (Table C1.) shows the errors of all particle distributions.

4. Discussion

4.1. Hydraulic model validation

Model performance that was associated with the gully pot discharges during each rainfall intensity was high, as R^2 values ranged between 0.93 and 0.96 and maximum NRMSE were 13 %. However, some of this error may have been attributable to surface flows interacting with the sidewalk. This was apparent during the physical experiments. Hence there was a small contribution of runoff from sidewalk to roadway, which was then received by the gully pots. This was particularly apparent for gully pot 2 in the physical model. Yet, the sidewalk was denied this connection throughout the numerical simulations. Model performance was slightly lower for gully pot 2 discharges than gully pot 1 due to this interaction. This was not considered too detrimental to the findings of this study due to accuracy of the numerical discharges being high.

Along similar lines the model performed well regarding velocity fields recorded within the sediment collection area. Here R^2 values were all above 0.90 for both the x and y fields for each rainfall intensity. When comparing these results to similar numerical studies that validated flows with experimental facility datasets, we confirm that it is a robust modelling outcome. For example, velocity field errors were similar during the studies conducted by Martins et al. (2018) and Addison-Atkinson et al. (2023). In both studies the majority of R^2 results were also above 0.90. However, both these studies found that modelled velocity fields in the longitudinal direction (x) had slightly better performance than in the lateral direction (y). Though in the current study x and y velocity field errors were homogeneous.

The largest hydraulic model NRMSE in this study was identified from the three depth locations at S7, S8 and S9. The discrepancies of simulated depths were between 15 % and 39 %, which is considered poor as the latter NRMSE was above the 30 % threshold of a good model (Gao et al., 2022). Though this was very likely to do with the depth measurements within the facility being associated with some uncertainty due to the difficulties of measuring extreme shallow flows (Naves et al., 2020a). So we believe this not to be bad agreement with the simulation outputs considering this uncertainty. Similarly, the depth errors did not affect the accuracy of gully pot discharges, nor velocity fields. Hong et al., (2016b) found in another study that depth simulations are more accurate, though have had far less uncertainty from the collected depth measurements. With regards to model error and rainfall intensity, the results showed that when the rainfall intensity increased model performance also increased. This is an interesting outcome that has also been replicated in other studies. For example, Chakravarti and Jain (2014) found that their rainfall runoff model was more accurate with a rainfall intensity of 90 mm/h than 30 mm/h.

4.2. Sediments collected in gully pots

Although there was some disparity to the modelled water depths as explained above, sediments collected in the gully pots were still adequately modelled. This meant that suspended load calculations, which rely on accurate flow depths, were still able to calculate sediment transport accurately. NRMSE were below 12 % for particle size distributions D2, D3 and D4. The results showed that the graded particle distribution (D5) had a much larger disparity from the validated model. Which was hypothesised and the NRMSE were as high as 61 % when using D_{50} as sediment characteristic diameter. This occurs due to the mechanics of sediment movement. That is, in graded sediments the

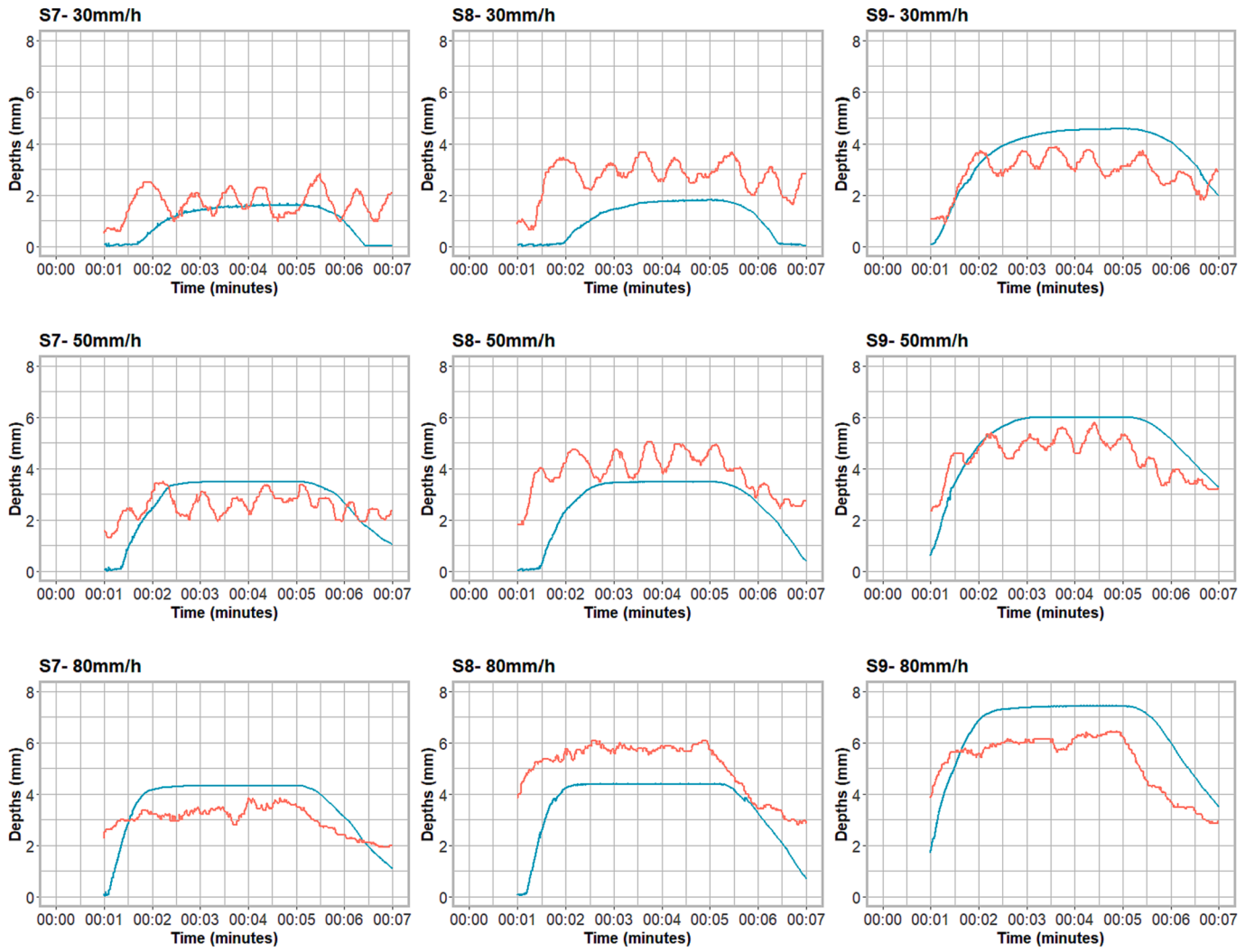

Fig. 3.3. Depths taken in the sediment collection area. The figure shows the three locations (S7, S8 and S9) with each rainfall scenario (30, 50 and 80 mm/h). The observed depths are shown in red, and the simulated depths are shown in blue. (For interpretation of the references to colour in this figure legend, the reader is referred to the web version of this article.)

settling velocities between the suspended and bed load sediments vary. Coarser bed load particles have a higher chance of entrainment because their contact to flow increases. As follows, for fine particles on the bed the circumstance is the opposite. Here fine particles are likely to be sheltered by the coarser ones (Wu et al., 2000). Which is the main reason for using different sediment diameters than D_{50}. This does depend on how fine the particles are, as other studies have found a different outcome. For example Zhao et al. (2018) identified from experimental and numerical analysis that finer particles (<105 μm) have a higher wash-off percentage than coarser particles. This is due to finer particles becoming suspended more easily, and therefore have a greater settling velocity than coarser particles. Zhao et al. (2018) also concluded that particle transport is greater on smoother concrete surfaces than asphalt. Asphalt will retain a larger number of sediments due to a higher depression storage. So, it is likely that in the current study wash-off rates are high due to the concrete surface used. The importance of sediment grading was also highlighted by Xiao et al. (2022) which demonstrates in small scale wash-off tests that the effect of sediment grading is crucial when sediment D_{50} is over 100 μm.

Previous studies have used correction factors to account for sediments mixing. For example, corrected shear stress (Fischer-Antze et al., 2009) and adaptation coefficients (Termini, 2014); which allows the simulation of sediment interchange between the bed and the stream and the variation of sediment size distribution in space and in time. In this current study the geometric mean (D_g) replaced the median grain size (D_{50}) of the graded sediment and was simulated. This meant that a value of 118.4 (μm) was used in the pre-processing instead of 165.3 (μm). The applicability of the van Rijn model, as stated by Wu et al., (2000) is for mean particle sizes between 200 and 2000 μm. Within MIKE21 FM the range of median diameters using the van Rijn model for non-cohesive sediments is $>$ 60 μm. The novelty of this study was to apply these smaller diameters with a good level of accuracy using the geometrical average for a graded sediment wash-off using a uniform sediment model. The non-graded sediments within this study have a very uniform granulometry. Thus, D_g and D_{50} were very similar, and the results did not significantly vary when using D_g for the uniform particle size distributions.

4.3. Main benefits and potentialities of study

A small constrain of this study was the inability to model cohesive particles that had a $D_{50} < 60$ μm with the sand transport model. For example, the data collected within the water facility of this study identified one particle distribution that fit this characteristic, namely D1 which had a $D_{50} = 30.1$ μm. MIKE21 FM can simulate cohesive particles, though this is done with a mud transport model. As such it was left out of

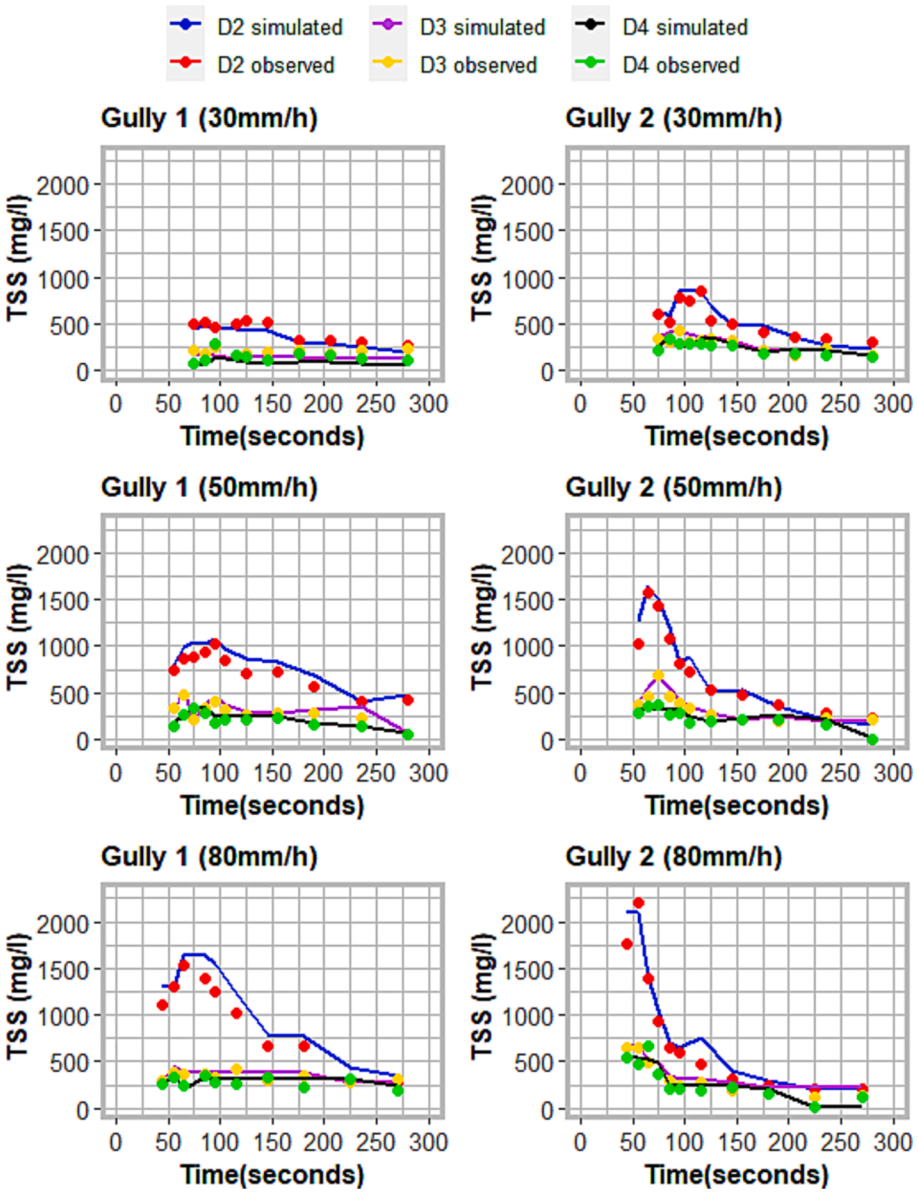

Fig. 3.4. Simulated and observed sediment wash-off into gully pot 1 and gully pot 2 of D2-D4 particle size distributions using their D_{50}. The figure illustrates total suspended solids (TSS mg/l) collected into each gully pot for each rainfall intensity scenario.

the analysis instead of using two different models. Secondly, the sidewalk was not included in the numerical simulations. A boundary was implemented which separated the interaction between rainfall and gully pots via sidewalk runoff. This was done to simplify the simulations and was considered agreeable as model performance was not unacceptably restricted.

Besides these constraints, we have shown that in our approach we have used a river sediment model to simulate sediment transport with uniform and graded particle size distributions working with D_g instead of D_{50}. This is in comparison to other methods available. Sediment wash-off phenomena has been widely studied since the inception of Sartor and Boyd (1972). Empirical wash-off equations, such as the developed by Sartor et al. (1974) and Egodawatta et al. (2007) consider an exponential equation which needs to be tuned by introducing empirical parameters related with sediment particle size distributions, rainfall intensity or surface roughness. On the other hand, the detailed modelling works of Hong et al. (2019) and Naves et al., (2020a) consider the physical phenomenon involved in the wash-off process based on Harsine-Rose sediment transport equations, but require calibration of up to six parameters, with limited knowledge still of their behaviour in urban catchments. Thus, the main difference of the proposed approach is that, once the hydraulic model is calibrated, the sediment transport model is straightforward to apply as just sediment density and sediment characteristic diameter (D_{50} or D_g, depending on the sediment gradation) are needed to obtain meaningful and accurate results. Thus, the application of this simpler river sediment transport equations might simplify the wash-off modelling for realistic applications in real urban catchments, although more research is needed to analyse their validity for different sediment sizes and for organic–inorganic sediment mixtures.

5. Conclusion

An experimental facility was used in this study for the collection of high-resolution datasets containing gully pot discharges, velocity fields, water depths and sediment wash-off to accurately validate a numerical model. A sand transport and hydraulic model was built in MIKE 21 FM. Simulations took place under three rainfall intensities (30, 50 and 80

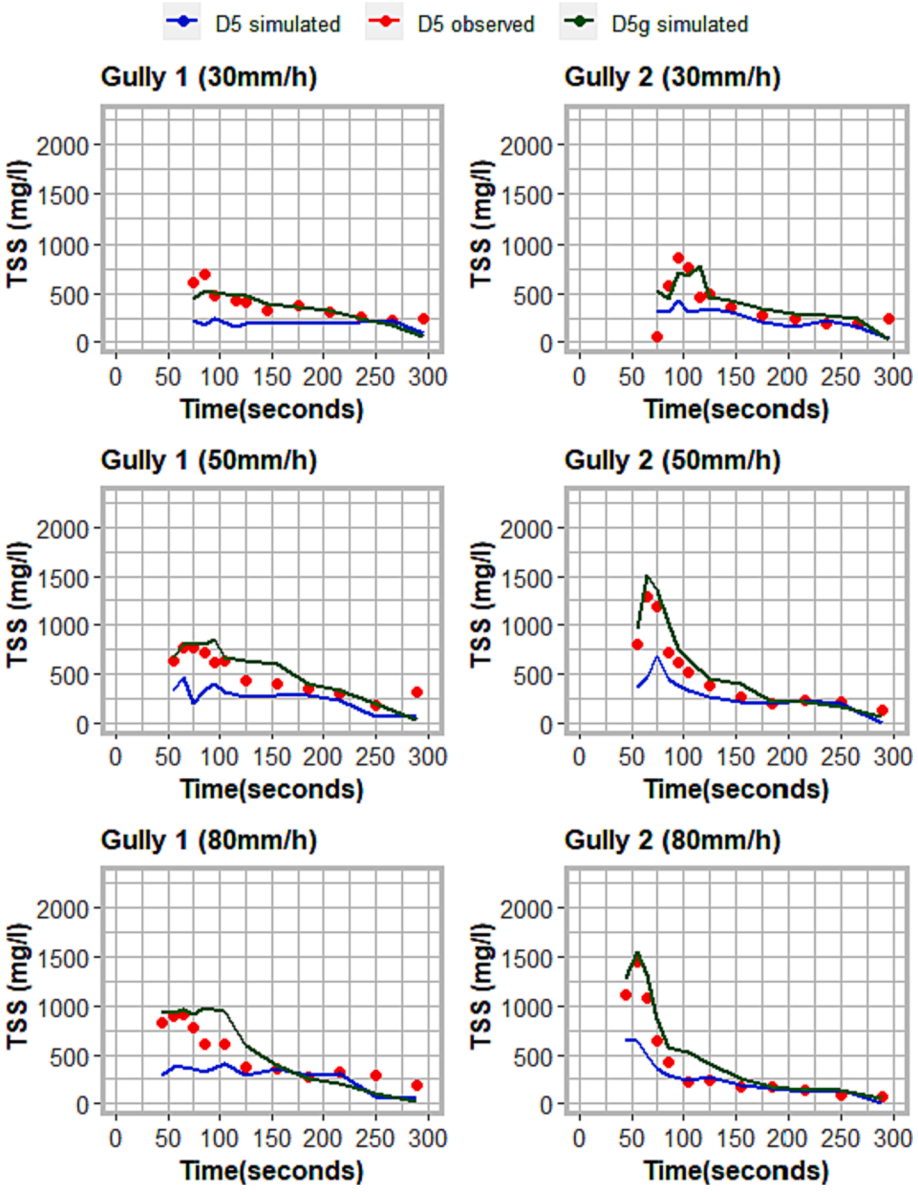

Fig. 3.5. Simulated and observed sediment wash-off into gully pot 1 and gully pot 2 with particle size distribution D5 using their D_{50} (D5 simulated), and with particle size D5 using the geometric mean ($D5_g$) The figure illustrates total suspended solids (TSS mg/l) collected into each gully pot for each rainfall intensity scenario.

mm/h). The model was able to replicate the wash-off and transport of uniform sediments to high standard when the output was compared to the experimental facility results. Yet, one question that this study investigated is the associated error regarding the simulation of graded sediment distributions. It was hypothesised that the model would not be able to simulate a graded sediment due to the way sediments of different sizes interact with each other under flow conditions. As a result, this study identified that instead of using median grain size (which was successful for simulating uniform sediments) it was more accurate using the geometric mean for a graded sediment. The conclusions can be simplified as follows:

Model validation of gully discharge, surface velocities fields and surface depths.

- Gully pot discharge NRMSE were low (between 12 % and 13 %) for all rainfall intensities. Model performance for gully pot 1 was higher than gully pot 2, due to the interaction of flow from the sidewalk to street surface in the experimental facility.
- Surface velocities were accurately simulated for both x and y fields (R^2 were above 0.9).
- Water depths in the sediment collection area had errors due to the uncertainty of rain generation. Error ranges were between 18 % and 39 %, with more error occurring in lower rainfall intensities.

Model validation of sediment wash-off.

- The geometrical mean for a graded sediment wash-off using a uniform sediment model was accurately applied.
- Model performance was high when simulating the wash-off and transport of uniform sediments. NRMSE were between 11 % and 12 %. Wash-off into gully pot 1 had slightly better model performance than gully pot 2.
- Model performance was low when simulating the wash-off and transport of a graded sediment when assigning the median as the sediment diameter. NRMSE were between 43 % and 61 %.

Table A1
R^2 values of gully pot discharges (Q) and surface velocities (m/s) from each rainfall event.

Rainfall (mm/h)	Location	Measurement type	Gully pot 1	Gully pot 2	Sediment collection area
30	Gully pot	Discharge (Q)	0.96	0.95	–
50			0.95	0.94	–
80			0.95	0.93	–
30	Surface	x velocity field (m/s)	–	–	0.92
50			–	–	0.91
80			–	–	0.91
30	Surface	y velocity field (m/s)	–	–	0.92
50			–	–	0.91
80			–	–	0.90

Table B1
Normalised root mean square error (NRMSE) of discharges (Q) into both gully pots, and at each depth location (S7, S8 and S9) for three rainfall intensities.

Rainfall (mm/h)	Gully pot 1	Gully pot 2	S7	S8	S9
30	0.12	0.13	0.37	0.39	0.23
50	0.12	0.13	0.22	0.24	0.15
80	0.13	0.13	0.21	0.21	0.18

Table C1
Normalised root mean square error (NRMSE) of sediment wash-off into both gully pots. Results are shown for median diameter (D_{50}) of the uniform sediments (D2-D4), and the graded sediment (D5). The geometric mean of D5 ($D5_g$) and the median diameters of the two fractions that were used to create D5 are also shown.

	Rainfall (mm/h)	D2 (D_{50})	D3 (D_{50})	D4 (D_{50})	D5 (D_{50})	$D5_g$ (D_g)
Gully pot 1	30	0.11	0.11	0.11	0.43	0.13
	50	0.11	0.11	0.11	0.47	0.13
	80	0.11	0.11	0.11	0.50	0.14
Gully pot 2	30	0.12	0.12	0.12	0.49	0.13
	50	0.12	0.12	0.12	0.53	0.13
	80	0.12	0.12	0.12	0.61	0.14

- Simulations that applied the geometric mean to the graded sediment simulations had less error when used as the grain diameter. Errors were between 13 % and 14 %.

CRediT authorship contribution statement

W. Addison - Atkinson: . **A.S. Chen:** Conceptualization, Supervision. **F.A. Memon:** Conceptualization. **J. Anta:** Conceptualization, Supervision. **J. Naves:** Conceptualization, Supervision. **L. Cea:** Conceptualization, Supervision.

Declaration of competing interest

The authors declare that they have no known competing financial interests or personal relationships that could have appeared to influence the work reported in this paper.

Data availability

Data will be made available on request.

Acknowledgment

The work presented in this paper was carried out as part of PhD research and was supported by the EPSRC Centre for Doctoral Training in Water Informatics Science and Engineering (WISE CDT; EP/L016214/1). The experimental part and data collection received funding from the Spanish Ministry of Science, Innovation and Universities under PORE-DRAIN project RTI2018-094217-B-C33 (MINECO/FEDER-EU). The authors would also like to thank the Danish Hydraulic Institute for supplying the academic license for the MIKE 21 model.

Appendix A

References

Addison-Atkinson, W., Chen, A.S., Rubinato, M., Memon, F.A., Shucksmith, J.D., 2023. Quantifying flood model accuracy under varying surface complexities. J. Hydrol. 620. May, p. 129511.
Beg, M., Rubinato, M., Carvalho, R., Shucksmith, J., 2020. CFD Modelling of the Transport of Soluble Pollutants from Sewer Networks to Surface Flows during Urban Flood Events. Water 12 (9), 2514.
Bui, V., Bui, M., Rutschmann, P., 2019. Advanced Numerical Modeling of Sediment Transport in Gravel-Bed Rivers. Water 11 (3), 550.
Butler, D., Digman, C., Makropoulos, C., Davies, J.W., 2018. Urban drainage. CRC Press, Taylor & Francis, Boca Raton.
Chakravarti, A., Jain, M., 2014. Experimental Invesitigation and Modeling of Rainfall Runoff Process. J. Sci. Technol. 7 (12).
Chang, H., Allen, D., Morse, J., Mainali, J., 2019. Sources of contaminated flood sediments in a rural–urban catchment: Johnson Creek, Oregon. J. Flood Risk Manage. 12 (4).
Darama, Y., Yılmaz, K., Melek, A.B., 2021. Land degradation by erosion occurred after irrigation development in the Harran plain, Southeastern Turkey. Environ. Earth Sci. 80 (6), 211.
Deletic, A., 2000. Modelling input of fine granular sediment into drainage systems via gully-pots. Water Res. 34 (15), 3836–3844.
Dhi, 2022. 'MIKE21 Model Manager. User guide, Danish Hydraulic Institute, Horsholm, Denmark. Available from https://manuals.mikepoweredbydhi.help/2017/MIKE_21.htm'.
Dhi, 2023. 'MIKE21 & MIKE 3 Flow Model. Model Manager. Scientific Documentation. Danish Hydraulic Institute, Horsholm, Denmark. Available from //https://manuals.mikepoweredbydhi.help/latest/Coast_and_Sea/MIKE_FM_ST_Scientific_Doc.pdf'.
Egodawatta, P., Thomas, E., Goonetilleke, A., 2007. Mathematical interpretation of pollutant wash-off from urban road surfaces using simulated rainfall. Water Res. 41 (13), 3025–3031.
Fischer-Antze, T., Rüther, N., Olsen, N.R.B., Gutknecht, D., 2009. Three-dimensional (3D) modeling of non-uniform sediment transport in a channel bend with unsteady flow. J. Hydraul. Res. 47 (5), 670–675.
Fraga, I., Cea, L., Puertas, J., 2017. Validation of a 1D–2D dual drainage model under unsteady part-full and surcharged sewer conditions. Urban Water J. 14 (1), 74–84.
Fujita, I., Muste, M., Kruger, A., 1998. Large-scale particle image velocimetry for flow analysis in hydraulic engineering applications. J. Hydraul. Res. 36 (3), 397–414.
Gao, G., Falconer, R.A., Lin, B., 2011. Numerical modelling of sediment–bacteria interaction processes in surface waters. Water Res. 45 (5), 1951–1960.
Gao, N., Mo, Y., Wang, J., Yang, L., Gong, S., 2022. Effects of Flow Path Geometrical Parameters on the Hydraulic Performance of Variable Flow Emitters at the Conventional Water Supply Stage. Agriculture 12 (10), 1531.
Hong, Y., Bonhomme, C., Le, M.-H., Chebbo, G., 2016a. A new approach of monitoring and physically-based modelling to investigate urban wash-off process on a road catchment near Paris. Water Res. 102. October, pp. 96–108.
Hong, Y., Bonhomme, C., Le, M.-H., Chebbo, G., 2016b. New insights into the urban washoff process with detailed physical modelling. Sci. Total Environ. 573. December, pp. 924–936.
Hong, Y., Liao, Q., Bonhomme, C., Chebbo, G., 2019. Physically-based urban stormwater quality modelling: An efficient approach for calibration and sensitivity analysis. J. Environ. Manage. 246. September, pp. 462–471.
Kesserwani, G., Lee, S., Rubinato, M. and Shucksmith, J. (2015) 'Experimental and numerical validation of shallow water flow around a surcharging manhole.' 10th International Urban Drainage Conference September 20-23 Quebec Canada, page 10 p. 10.
Le Boursicaud, R., Pénard, L., Hauet, A., Thollet, F., Le Coz, J., 2016. Gauging extreme floods on YouTube: application of LSPIV to home movies for the post-event determination of stream discharges: Application of LSPIV to Flood Home Movies. Hydrol. Process. 30 (1), 90–105.
Leitão, J.P., Peña-Haro, S., Lüthi, B., Scheidegger, A., Moy de Vitry, M., 2018. Urban overland runoff velocity measurement with consumer-grade surveillance cameras and surface structure image velocimetry. J. Hydrol. 565. October, pp. 791–804.
Liu, Y., Sansalone, J.J., 2020. Physically-Based Particle Size Distribution Models of Urban Water Particulate Matter. Water Air Soil Pollut. 231 (11), 555.
Maike, W., Nina, V., Rainer, M., 2019. The Efficiency of Storm Water Sedimentation Tanks for Fine Particles in Urban Run-off. In: Mannina, G. (Ed.), New Trends in Urban Drainage Modelling. Springer International Publishing (Green Energy and Technology), Cham, pp. 854–858.

Martins, R., Kesserwani, G., Rubinato, M., Lee, S., Leandro, J., Djordjević, S., Shucksmith, J.D., 2017. Validation of 2D shock capturing flood models around a surcharging manhole. Urban Water J. 14 (9), 892–899.
Martins, R., Rubinato, M., Kesserwani, G., Leandro, J., Djordjevic, S., Shucksmith, J.D., 2018. On the Characteristics of Velocities Fields in the Vicinity of Manhole Inlet Grates During Flood Events. Water Resour. Res. 54 (9), 6408–6422.
Murali, M.K., Hipsey, M.R., Ghadouani, A., Yuan, Z., 2019. The development and application of improved solids modelling to enable resilient urban sewer networks. J. Environ. Manage. 240. June, pp. 219–230.
Muthusamy, M., Tait, S., Schellart, A., Beg, M.N.A., Carvalho, R.F., de Lima, J.L.M.P., 2018. Improving understanding of the underlying physical process of sediment wash-off from urban road surfaces. J. Hydrol. 557. February, pp. 426–433.
Naves, J., Jikia, Z., Anta, J., Puertas, J., Suárez, J., Regueiro-Picallo, M., 2017. Experimental study of pollutant washoff on a full-scale street section physical model. Water Sci. Technol. 76 (10), 2821–2829.
Naves, J., Anta, J., Puertas, J., Regueiro-Picallo, M., Suárez, J., 2019a. Using a 2D shallow water model to assess Large-Scale Particle Image Velocimetry (LSPIV) and Structure from Motion (SfM) techniques in a street-scale urban drainage physical model. J. Hydrol. 575, 54–65.
Naves, J., Anta, J., Suárez, J., Puertas, J., 2019b. WASHTREET - Hydraulic, wash-off and sediment transport experimental data obtained in an urban drainage physical model. Zenodo.
Naves, J., Rieckermann, J., Cea, L., Puertas, J., Anta, J., 2020a. Global and local sensitivity analysis to improve the understanding of physically-based urban wash-off models from high-resolution laboratory experiments. Sci. Total Environ. 709, 136152.
Naves, J., Anta, J., Suárez, J., Puertas, J., 2020b. Development and Calibration of a New Dripper-Based Rainfall Simulator for Large-Scale Sediment Wash-Off Studies. Water 12 (1), 152.
Pradhan, U.K., Mishra, P., Mohanty, P.K., Panda, U.S., Ramanamurthy, M.V., 2020. 'Modeling of tidal circulation and sediment transport near tropical estuary, east coast of India'. Regional Studies in Marine. Science 37, May, 101351.
Rietveld, M.W.J., Clemens, F.H.L.R., Langeveld, J.G., 2020. Monitoring and statistical modelling of the solids accumulation rate in gully pots. Urban Water J. 17 (6), 549–559.
Rubinato, M., Martins, R., Kesserwani, G., Leandro, J., Djordjevic, S. and Shucksmith, J. (2017) 'Experimental calibration and validation of sewer/surface flow exchange equations in steady and unsteady flow conditions.' *Journal of Hydrology*, 552, September, pp. 421–432.
Rubinato, M., Lee, S., Martins, R., Shucksmith, J.D., 2018. Surface to sewer flow exchange through circular inlets during urban flood conditions. J. Hydroinf. 20 (3), 564–576.
Rubinato, M., Helms, L., Vanderlinden, M., Hart, J., Martins, R., 2022. Flow exchange, energy losses and pollutant transport in a surcharging manhole linked to street profiles. J. Hydrol. 604, January, 127201.
Sartor, J.D., Boyd, G.B., Agardy, F.J., 1974. Water pollution aspects of street surface contaminants. J. Water Pollut. Control Fed. 3 (46).
Sravanthi, N., Ramakrishnan, R., Rajawat, A.S., Narayana, A.C., 2015. Application of Numerical Model in Suspended Sediment Transport Studies along the Central Kerala, West-coast of India. Aquat. Procedia 4, 109–116.
Termini, D., 2014. Non-uniform Sediment Transport Estimation in Non-equilibrium Situations: Case Studies. Procedia Eng. 70, 1639–1648.
Wu, W., Wang, S.S.Y., Jia, Y., 2000. Nonuniform sediment transport in alluvial rivers. J. Hydraul. Res. 38 (6), 427–434.
Xiao, Y., Luan, B., Zhang, T., Liang, D., Zhang, C., 2022. Experimental study of sediment wash-off process over urban road and its dependence on particle size distribution. Water Sci. Technol. 86 (10), 2732–2748.
Zavattero, E., Du, M., Ma, Q., Delestre, O., Gourbesville, P., 2016. 2D Sediment Transport Modelling in High Energy River – Application to Var River, France. Procedia Eng. 154, 536–543.
Zhang, T., Xiao, Y., Liang, D., Tang, H., Yuan, S. and Luan, B. (2020) 'Rainfall Runoff and Dissolved Pollutant Transport Processes Over Idealized Urban Catchments.' *Frontiers in Earth Science*, 8, July, p. 305.
Zhao, H., Jiang, Q., Xie, W., Li, X., Yin, C., 2018. Role of urban surface roughness in road-deposited sediment build-up and wash-off. J. Hydrol. 560, May, 75–85.